MAGNETIC RESONANCE IN CHEMISTRY, VOL. 35, 363–366 (1997)

^{119}Sn Solid-State NMR of Tin Sulfides. Evidence of Polytypism in SnS_2

Tanja Pietrass* and Francis Taulelle
RMN et Chimie du Solide, UMR 50, Université Louis Pasteur–Bruker–CNRS, 4 rue Blaise Pascal, 67070 Strasbourg Cedex, France

The ^{119}Sn magic angle spinning NMR spectra of the three tin sulfides SnS, SnS_2 and Sn_2S_3 are discussed with respect to results from x-ray structure analysis. The distortion from an octahedral environment of tin in SnS and Sn(II) in Sn_2S_3 is reflected in the large chemical shift anisotropy. The denser coordination sphere of Sn(IV) in SnS_2 in comparison with Sn_2S_3 is reflected in the upfield shift observed for SnS_2. With the same argument, the shift of Sn(II) in the sulfides under study is generally much lower than that of Sn(IV). The ^{119}Sn high-resolution solid-state NMR signal of SnS_2 displays a fine structure which is assigned to different polytypic regions in the crystallites. © **1997 by John Wiley & Sons, Ltd.**

Magn. Reson. Chem. **35**, 363–366 (1997) No. of Figures: 2 No. of Tables: 1 No. of References: 20

Keywords: NMR; ^{119}Sn NMR; tin sulfides; solid state

Received 18 June 1996; revised 14 November 1996; accepted 18 November 1996

INTRODUCTION

^{119}Sn high-resolution NMR has been applied to elucidate the structure and dynamics of a variety of materials, mainly organotin compounds[1–5] and tin oxides[6,7] for catalytic applications.[8]

In the framework of a structural study of lithium-intercalated SnS_2 compounds,[9] we investigated the effects of structural and electronic changes on the tin nucleus in a series of tin sulfides (SnS, Sn_2S_3, SnS_2) by ^{119}Sn solid-state NMR spectroscopy. For SnS_2, there are 21 polytypes reported in the literature determined by x-ray crystallography.[10–12] Using powder x-ray analysis, the different polytypes cannot be distinguished. One aspect of this work is to show that polytypism in powders can be evidenced by solid-state NMR spectroscopy.

EXPERIMENTAL

^{119}Sn magic angle spinning (MAS) NMR spectra were recorded on a Bruker MSL 300 NMR spectrometer at a Larmor frequency of 111.921 MHz. Samples were packed in ZrO_2 rotors of 4 mm o.d. Chemical shift anisotropies were estimated with the program Winfit (Bruker) and determined for two different spinning speeds (3 and 12 kHz). For SnS_2, only the value obtained at a spinning frequency of 3 kHz is reported. For SnS, the values obtained at different speeds were consistent. A lower limit for the value of Sn_2S_3 was estimated from the distribution of sidebands. Isotropic chemical shifts were determined by comparing MAS spectra at different spinning speeds. Chemical shifts are reported using the convention that higher frequencies correspond to a more positive chemical shift value.

* *Correspondence to*: T. Pietrass. Present address: Department of Chemistry, New Mexico Institute of Mining and Technology, Socorro, NM 87801, USA.

RESULTS AND DISCUSSION

Figure 1 shows the ^{119}Sn MAS NMR spectra of the tin sulfides SnS, Sn_2S_3 and SnS_2. The spectrum of SnS is split up into a set of rotational sidebands with an isotropic chemical shift $\delta_{iso} = -299$ ppm and a chemical shift anisotropy $\delta_{CSA} = -384$ ppm. The ^{119}Sn NMR spectrum of SnS_2 shows a single peak at -763 ppm. On lowering the spinning speed to 3.5 kHz, the chemical shift anisotropy could be determined from the rotational sideband pattern as $\delta_{CSA} = -79$ ppm. A

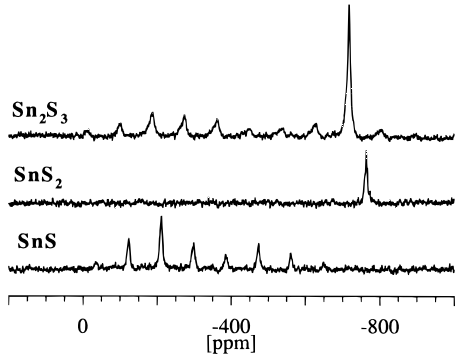

Figure 1. ^{119}Sn MAS NMR of the three tin sulfides SnS, SnS_2 and Sn_2S_3. MAS spinning frequency, 10 kHz; spectral width, 250 kHz; pulse width, 4 μs; recycle delay, 5 s; SnS, 1000 transients; SnS_2, 400 transients; Sn_2S_3, 7808 transients.

 CCC 0749–1581/97/060363–04 $17.50

superposition of the spectra of SnS and SnS_2 corresponds roughly to the spectrum of Sn_2S_3. However, the peak corresponding to Sn(IV) is shifted slightly downfield to $\delta_{iso} = -719$ ppm.

Whereas in SnS_2 each Sn atom is in a highly symmetric environment,[13] the symmetry in SnS is much lower.[14] Each tin atom in SnS_2 is surrounded by a hexagon of tin atoms located in the same plane. The sulfur atoms form an octahedral environment around each tin atom, with three sulfur atoms located above and below the tin plane. The Sn—S bond length is 2.56 Å. Different stacking of the SnS_2 layers gives rise to a large number of polytypes.[11,12] The layers are held together by van der Waals forces with a spacing of 3.65 Å. In SnS, each tin atom is also surrounded by six sulfur atoms, but in a highly distorted octahedral arrangement due to the stereochemically active lone pair on Sn(II). The SnS molecules form layers in which each tin atom has three almost equally distant sulfur neighbors (2.66, 2.66 and 2.62 Å) forming a trigonal pyramid with the tin atom at the apex. The other three sulfur atoms coordinating each tin atom belong to a neighbouring layer, resulting in longer Sn—S distances (3.29, 3.29 and 3.39 Å). The layers are linked together by weak Sn—S···Sn and Sn···Sn interactions.[11,12]

The highly distorted octahedral environment causes the large chemical shift anisotropy observed for Sn(II). The smaller isotropic chemical shift value of SnS compared with SnS_2 indicates a lower shielding of the Sn(II) nucleus in SnS when compared with Sn(IV). It has been shown that an increase in the coordination number of tin leads to a stronger shielding of the tin nucleus, that is, an upfield shift (lower frequency).[15,16] The short bond lengths in SnS_2 (2.56 Å) create a denser coordination sphere around the tin nucleus than in SnS, where the octahedron is highly distorted owing to the considerable increase in three of the bond lengths. Thus, a downfield shift is expected for Sn(II), which is in agreement with the experimental result.

In Sn_2S_3, which is better described as a mixed sulfide $SnS_2 \cdot SnS$, there are two types of tin atoms in the structure. The Sn(IV) atoms are located in the centers of slightly distorted octahedra formed by the sulfur atoms. The Sn(IV)—S bond lengths range from 2.50 to 2.61 Å.[17,18] The octahedra form infinite double rutile strings with the Sn(II) atoms attached laterally. As in SnS, the Sn(II) atoms in Sn_2S_3 occupy the apical position in a trigonal pyramid. The Sn(II)—S bond lengths in Sn_2S_3 are 2.64, 2.64 and 2.74 Å.

One of the bond angles of the Sn(II) atom in Sn_2S_3 formed with the three sulfur atoms of the trigonal pyramid is considerably smaller (83.6°) than the corresponding angle in SnS (86.8°), whereas the other S—Sn—S bond angle of the pyramid is similar in both compounds (90.2° in Sn_2S_3 and 89.0° in SnS).[14,17] A decrease in bond angle is frequently accompanied by a downfield shift.[19] Therefore, a decrease in the chemical shift of the Sn(II) peak in Sn_2S_3 is expected compared with SnS. In fact, the isotropic chemical shift value of Sn(II) in Sn_2S_3 is $\delta_{iso} = -274$ ppm compared with -299 pm in SnS. The chemical shift anisotropy of Sn_2S_3 is more than -800 ppm and thus substantially larger than that in SnS. This is in agreement with the distortion of the bond angles compared with SnS. Analogously, the isotropic chemical shift value of Sn(IV) in Sn_2S_3 is $\delta_{iso} = -719$ ppm, whereas for SnS_2 a value of -764 ppm has been found. This result indicates a decrease in the bond angle of Sn(IV) in Sn_2S_3 compared with SnS_2 which is in agreement with the results from x-ray structure analysis. The S—Sn—S bond angles on the Sn(IV) in Sn_2S_3 are 86.1°, 86.7° and 90.8°,[18] whereas SnS_2 presents a perfect octahedral arrangement with 90° bond angles.[11]

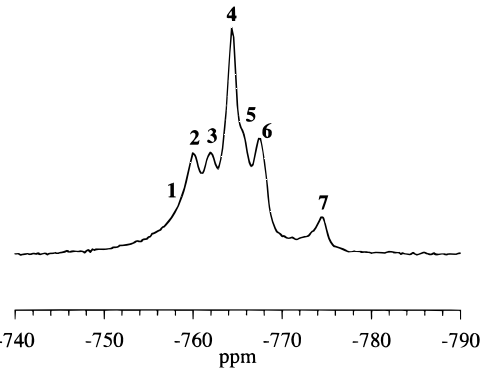

Figure 2. ^{119}Sn MAS NMR of SnS_2. MAS frequency, 12 kHz; spectral width, 50 kHz; pulse width, 2.8 μs; recycle delay, 5 s; 2880 transients. Peak positions are marked as in Table 1.

In conclusion, the high-resolution ^{119}Sn NMR spectra for the three sulfides agree well with their x-ray structures. However, a closer investigation of the Sn(IV) peak in SnS_2 reveals a fine structure (Fig. 2). The decomposition into individual Lorentzian lines is reported in Table 1. Several possibilities may account for the observed fine structure: (i) misadjustment of the magic angle, (ii) ^{119}Sn–^{119}Sn or ^{119}Sn–^{117}Sn J-coupling or (iii) different tin sites with slightly different chemical shifts. Possibility (i) can be ruled out. Similar splittings should also be observable for the other tin sulfides, since the magic angle was not readjusted when changing the sample. Possibility (ii) cannot be ruled out completely. In the tin planes, each tin atom is connected to its neighboring tin atoms via two bonds through the shared sulfur atoms at the corners of the octahedra. For

Table 1. ^{119}Sn chemical shifts of the different components of the SnS_2 signal (compare Fig. 2)[a]

Peak component, n	Chemical shift (ppm)	Peak distance, $(n+1)-n$ (Hz)
1	−757.7	
2	−759.9	266
3	−761.9	223
4	−764.4	275
5	−765.8	157
6	−767.5	196
7	−774.4	771

[a] Chemical shifts were obtained by decomposition into different Lorentzians. The last column gives the energy differences between the individual peak components.

^{119}Sn, ^{2}J-couplings are generally in the region of 10^2 Hz. For example, in $(Me_3Sn)_4C$, a value of $^{2}J = 328$ Hz is reported.[1] For a coupling through a chalcogen such as oxygen, $^{2}J = 74$ Hz was found in $(n\text{-}Bu_2ClSn)_2O$.[10]

It is evident from Table 1 that the frequency differences between the individual peaks are of the order of 10^2 Hz. If all the tin atoms were equivalent as predicted from the x-ray structure, a $^{2}J(^{119}Sn–^{119}Sn$ or $^{119}Sn–^{117}Sn)$ should give rise to only one set of satellite lines for each of the isotope pairs. The ratio of the intensities of these satellites to the central (uncoupled) peak can be much larger than just the ratio of the natural abundances, since each tin atom is surrounded by six other tin atoms. The corresponding J values should then reflect the ratio of the nuclear gyromagnetic ratios γ with $\gamma(^{119}Sn)/\gamma(^{117}Sn) = 1.0465$. However, the observed pattern is more complex and, thus, requires the presence of different tin sites. Each tin nucleus at a specific site can couple with up to six neighboring tin nuclei whose identity as ^{119}Sn or ^{117}Sn follows a statistical distribution according to their natural abundances. In order to verify the possibility of overlapping multiplet structures caused by tin atoms at different sites and subject to scalar coupling, a ^{117}Sn NMR spectrum was recorded under conditions identical with those for ^{119}Sn. Since both J-coupling and chemical shift scale with the gyromagnetic ratios, the peak positions are expected to be identical in both spectra with the exception of peaks arising from $^{119}Sn–^{119}Sn$ or $^{117}Sn–^{117}Sn$ J-coupling. However, since the abundances of both tin isotopes differ by 12%, the peak intensities should vary for peaks arising from scalar coupling. No such change was observed. Moreover, in the experimentally observed pattern, each of the spacings between the individual components is unique and cannot be attributed to a multiplet structure. The most intriguing evidence, however, that the observed pattern is not generated by pure J-coupling, is the change in the relative intensities of the individual peaks upon chemical lithium insertion, which does not cause a shift of the resonance lines.[9]

Therefore, we conclude that J-coupling is not a dominant mechanism, and the fine structure of the Sn(IV) peak in SnS_2 is mainly due to tin atoms in a slightly different environment generating small chemical shift differences [possibility (iii)]. Slight changes in the environment of the tin nuclei may be caused by regions in the crystallites of different polytypic structure.

Polytypism arises from different ways of stacking compatible units. The layer transposition–disorder theory provides an explanation for the formation and coexistence of polytypes. In SnS_2, two possible glide processes exist: S/S glide of low energy between the weakly bonded neighbouring planes of sulfur atoms, and Sn/S glide of higher energy occurring within the multiple layers themselves.[11] In a geometrical model of polytypism, the individual layers preserve their structure in all stacking sequences.[13] Several SnS_2 polytypes exist with hexagonal (H type) and rhombohedral (R type) symmetry. The basic polytypes in SnS_2 are 2H, 4H and 18R, respectively, and the most common stacking sequences are 2H and 18R.[20] Numerous combinations of stacking sequences of the three basic polytypes exist. Large period polytypes occur in all small regions of the crystals.[10] Powder x-ray diffraction of our SnS_2 sample only revealed the reflections typical of the 2H polytype. It has been shown, however, that the powder x-ray diffraction pattern of crushed single crystals of different polytypic structure gave rise only to the reflections characteristic of the 2H structure.[11] Therefore, x-ray powder diffractometry is evidently not sensitive to the detection of coexisting polytypes in SnS_2.

NMR, however, a technique sensitive to local structural changes, enabled us to detect the coexistence of different polytypes in SnS_2. Different stacking periodicities give rise to different internuclear distances between the layers and the atoms therein, thus creating the small changes in the chemical environment of the tin nuclei as evidenced in different chemical shifts by ^{119}Sn high-resolution solid-state NMR.

CONCLUSIONS

The ^{119}Sn NMR isotropic chemical shifts and chemical shift anisotropies agree well with the x-ray structure results. For SnS_2, however, a fine structure of the Sn(IV) peak has been assigned to regions in the crystallites which are defined by different stacking periodicities in the layers. Although the powder x-ray diffraction pattern presents only the typical reflections of an SnS_2 2H structure, the sensitivity of high-resolution solid-state NMR allows the detection of local deviations from the long-range order.

Acknowledgements

The authors express their gratitude to P. Lavela, J.-C. Jumas and J. Olivier-Fourcade for providing the samples and to A. Pines for the use of a spectrometer.

REFERENCES

1. R. K. Harris, T. N. Mitchell and G. J. Nesbitt, *Magn. Reson. Chem.* **23**, 1080 (1985).
2. B. Wrackmeyer and E. Kupče, *Magn. Reson. Chem.* **29**, 260 (1991).
3. B. Wrackmeyer and E. Kupče, *Magn. Reson. Chem.* **30**, 964 (1992).
4. B. Wrackmeyer, E. Kupče and J. Kümmerlen, *Magn. Reson. Chem.* **30**, 403 (1992).
5. H. Bai and R. K. Harris, *J. Magn. Reson.* **96**, 24 (1992).
6. C. Cossement, J. Darville, J.-M. Gilles, J. B. Nagy, C. Fernandez and J.-P. Amoureux, *Magn. Reson. Chem.* **30**, 263 (1992).
7. N. J. Clayden, C. M. Dobson and A. Fern, *J. Chem. Soc., Dalton Trans.* 843 (1989).
8. T.-C. Sheng, P. Kirszensztejn, T. N. Bell and I. D. Gay, *Catal. Lett.* **23**, 119 (1994).
9. T. Pietrass, F. Taulelle, C. Bousquet, J. Olivier-Fourcade, J. C. Jumas and S. Steuernagel, submitted for publication.

10. R. S. Mitchell, Y. Fujiki and Y. Ishizawa, *Nature* (*London*) **247**, 537 (1974).
11. C. R. Whitehouse and A. A. Balchin, *J. Cryst. Growth* **47**, 203 (1979).
12. B. Palosz, W. Palosz and S. Gierlotka, *Acta Crystallogr., Sect. C* **41**, 807 (1985).
13. B. Palosz, W. Steurer and H. Schulz, *Acta Crystallogr., Sect. B* **46**, 449 (1990).
14. S. d. Bucchia, J.-C. Jumas and M. M. Maurin, *Acta Crystallogr., Sect. B* **37**, 1903 (1981).
15. S. J. Blunden, D. Searle and P. J. Smith, *Inorg. Chim. Acta* **116**, L31 (1986).
16. J. J. Burke and P. C. Lauterbur, *J. Am. Chem. Soc.* **83**, 326 (1961).
17. R. Kniep, D. Mootz, U. Severin and H. Wunderlich, *Acta Crystallogr., Sect. B* **38**, 2022 (1982).
18. D. Mootz and H. Puhl, *Acta Crystallogr* **23**, 471 (1967).
19. J. D. Kennedy, W. McFarlane and G. S. Pyne, *Bull. Soc. Chim. Belg.* **84**, 289 (1975).
20. T. Minagawa, *J. Phys. Soc. Jpn.* **49**, 2317 (1980).

